CHAPTER V

A NEW ALTERNATIVE FOR THE SMECTIC A_1 – REENTRANT NEMATIC – SMECTIC A_d BICRITICAL POINT

5.1 INTRODUCTION

As discussed previously in Chapter III, materials with a strongly polar end group exhibit a variety of A phases,' namely, the monolayer (A_1) phase, the partially bilayer (A_d) phase, the bilayer (A_2) phase and the incommensurate (A_{ic}) phase.[2] Transitions involving various forms of A phases[3-5] are also known. From symmetry arguments[6] both $A_d - A_1$ and $A_d - A_2$ transitions can only be first order while the $A_1 - A_2$ transition can be either first or second order[5] owing to the doubling of the lattice periodicity.[7]

The phenomenological theory developed by Prost[8,9] and later improved upon by Prost and Barois[10] has been successful in explaining the smectic A polymorphism. Two order parameters $\rho(r)$, the centre of mass density and $\phi(r)$, the dipolar order parameter associated with the head to tail correlation of the polar molecules are considered in expressing the Landau free energy in this theory. This theory which considers contributions up to third order also predicts the existence of A_{ic} phase whose occurrence has been established experimentally. Barois, Prost and Lubensky[6] have recently further extended the phenomenological theory by consider-

ing the fourth order terms in the Landau expansion of the free energy. With this modification of the free energy Barois et al.[6] have investigated the various possible phase diagrams that can be deduced within the framework of mean field theory. In the following section we shall briefly summarise the important theoretical aspects concerning the smectic A_1 - reentrant nematic - smectic A_d ($A_1 - N_{re} - A_d$) bicritical pdint and also the experimental aspects concerning this point. Finally in section 5.3 we shall describe the results of our experiments near an expected $A_1 - N_{re} - A_d$ bicritical point.

5.2 THE PHENOMENOLOGICAL THEORY

The fundamental aspects of this theory have been stated in Chapter III. A good description of the smectic A phase (of strongly polar materials) with two competing lengths essentially involves two order parameters

$$\phi(r) = \mathrm{Re}[\psi_1(r)]$$

$$\rho(r) = \mathrm{Re}[\psi_2(r)]$$

where $\psi_1(r)$ and $\psi_2(r)$ are complex fields.

$$\psi_1(r) = \psi_1 \exp(iq_p \cdot r)$$

$$\psi_2(r) = \psi_2 \exp(iq_\rho \cdot r)$$

In terms of these fields, the Landau-Ginzburg free energy of the

Prost model in d-dimensions is

$$\Delta f_s = \int d^d r \Big[\frac{1}{2} r_1 |\psi_1|^2 + \frac{1}{2} C_1 |(\nabla^2 + K_1^2)\, \psi_1|^2 + \frac{1}{2} D_1 |\nabla_\perp \psi_1|^2 + \frac{1}{2} r_2 |\psi_2|^2 + \frac{1}{2} C_2 |(\nabla^2 + K_2^2)\psi_2|^2 + \frac{1}{2} D_2 |\nabla_\perp \psi_2|^2 + D_{12}\, \mathrm{Re}\, \psi_1^2 \psi^*{}_2 + \frac{B_1}{4} |\psi_1|^4 + \frac{B_2}{4} |\psi_2|^4 + \frac{B_{12}}{2} |\psi_1|^2 |\psi_2|^2 \Big] \qquad (1)$$

where $r_1 = a_1(T - T_{1c})$ and $r_2 = a_2(T - T_{2c})$ measure the temperature from the noninteracting mean field transition temperatures T_{1c} and T_{2c} of the fields ψ_1 and ψ_2. $\nabla_\perp$ is a derivative in the plane perpendicular to the Z-axis, parallel to $\vec{n}$. The elastic terms $|(\nabla^2 + K_1^2)\, \psi_1|^2$ and $|(\nabla^2 + K_2^2)\psi_2|^2$ in equation 1 favour $q_p^2 = K_1^2$ and $q_p^2 = K_2^2$. The terms $\mathrm{Re}\, \psi_1^2 \psi^*_2$ favours lock-in at $q_p = 2q_p$.

To study the mean field phase diagram of linearly modulated phases, Barois et al.[6] choose q_p and q_p parallel to $\vec{n} = \hat{e}_z$ and seek spatially independent fields

$$\psi_1(r) = |\psi_1|$$

$$\psi_2(r) = |\psi_2|$$

which minimize Δf_s. It is clear then that one can expect the following phases :

1) the nematic phase (N) with $|\psi_1| = |\psi_2| = 0$,

2) the monolayer smectic phase (SA_1) with $|\psi_1| = 0$, $|\psi_2| \neq 0$, $q_p = K_2$, and

3) the bilayer antiferroelectric smectic phase (**SA**2) with

$$|\psi_1| \neq 0, \ |\psi_2| \neq 0 \quad \text{and} \quad q_p = \frac{1}{2} q_\rho = q_0 \ .$$

It should be remarked here that an antiferroelectric smectic A phase with no long range mass density modulation ($|\psi_1| \neq 0$, $|\psi_2| = 0$) is never stable because a non-zero $|\psi_1|$ always generates a nsn-zero $|\psi_2|$ via the third order term in Δfs .

The mean field free energy density of the N phase is zero, i.e.,

$$f_N = 0 \ .$$

The free energy density of the SA_1 phase is obtained by minimizing

$$F_{A_1} = (\tfrac{1}{2}) \, r_2 |\psi_2|^2 + \frac{B_2}{4} |\psi_2|^4$$

with respect to $|\psi_2|$ to yield

$$f_{A_1} = \begin{cases} 0 & r_2 > 0 \\ -\dfrac{r_2^2}{16 B_2} & r_2 < 0 \ . \end{cases}$$

The free energy density of the bilayer **SA**2 phase is obtained by minimizing

$$f_{A_2}(|\psi_1|, |\psi_2|, q_0) =$$

$$\frac{1}{2}[r_1 + C_1(q_0^2 - K_1^2)^2]|\psi_1|^2 + \frac{1}{2}[r_2 + C_2(4q_0^2 - K_2^2)^2]|\psi_2|^2$$

$$- D_{12}|\psi_1|^2|\psi_2| + \frac{B_1}{4}|\psi_1|^4 + \frac{B_2}{4}|\psi_2|^4 + \frac{B_{12}}{2}|\psi_1|^2|\psi_2|^2 \qquad (2)$$

with respect to $|\psi_1|$, $|\psi_2|$ and q_0. Minimization with respect to q_0 results in

$$q_0^2 \equiv \bar{q}_0^2 = \frac{C_1|\psi_1|^2 K_1^2 + 4C_2|\psi_2|^2 K_2^2}{C_1|\psi_1|^2 + 16C_2|\psi_2|^2}$$

To proceed with the algebraically complex minimization with respect to $|\psi_1|$ and $|\psi_2|$, Barois, Prost and Lubensky introduced

$$0, = 2\frac{D_{12}}{B_{12}}(C_2/C_1)^{1/2} x \cos\theta$$

$$2 = \frac{1}{2}\frac{D_{12}}{B_{12}} x \sin\theta$$

so that $\bar{q}_0^2 = K_1^2 \cos^2\theta + \frac{1}{4}K_2^2 \sin^2\theta$,

where x measures the degree of order and θ the relative amplitudes of ψ_1 and ψ_2. In terms of these variables the free energy density becomes

$$f(x,\theta) = x^2(y_1 \cos^2\theta + y_2 \sin^2\theta + z^2 \cos^2\theta \sin^2\theta)$$

$$- 2x^3 \cos^2\theta \sin\theta + x^4(1 + \delta B_1 \cos^4\theta + \delta B_2 \sin^4\theta), \qquad (3)$$

where

$$y_1 = 2\frac{B_{12}}{D_{12}^2} r_1 , \quad y_2 = \frac{1}{8}\frac{C_1}{C_2}\frac{B_{12}}{D_{12}^2} r_2 ,$$

$$z^2 = \frac{2C_1 B_{12}}{D_{12}^2}(K_1^2 - \frac{1}{4}K_2^2)^2 , \quad \delta B_1 = \frac{16B_1}{B_{12}}\frac{C_2}{C_1} - 1$$

$$\delta B_2 = \frac{1}{16}\frac{B_2}{B_{12}} - 1 .$$

Here y_1 and y_2 are the temperature variables and z^2 is the incommensurability parameter measuring the degree of phase mismatch between K_1 and $K_2/2$. The usual stability conditions demand δB_1 and δB_2 to be greater than -1. Numerical calculations performed by Barois, Prost and Lubensky to minimize the free energy have led to a variety of theoretical phase digrams. We will consider here a few which are most relevant to our experiments.

Case 1

A small incommensurability parameter with symmetric elastic and fourth order terms ($\delta B_1 = 6 B_2$) results in a phase diagram (see Fig. 5.1) which resembles the mean field N - SA_1 - SA_2 diagram

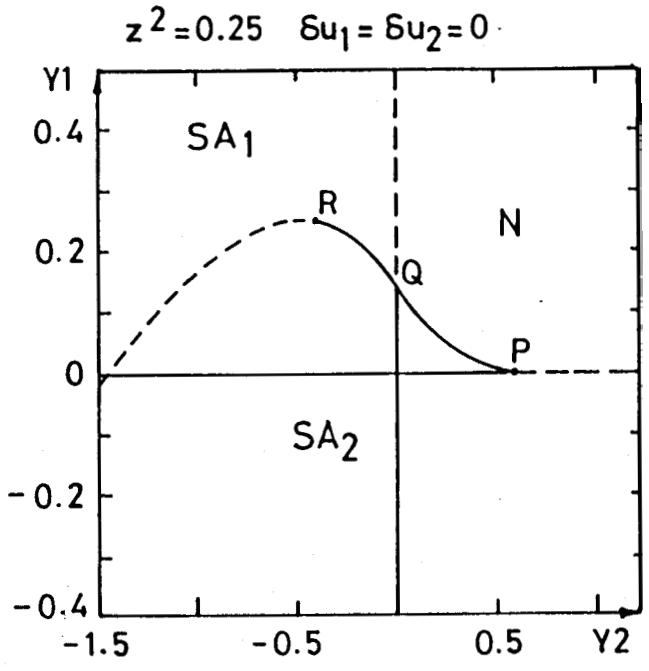

Figure 5.1

Phaoe diagram in the Y_1-Y_2 plane for a small incommensuzability pazameter (Z^2) with oymmetric elastic and fourth order tezmo (i.e., $\delta u_1 = \delta u_2 = 0$. The oolid line denotes a first-order phase boundary, while the daohed line denotes a oecond order boundary. (From Ref. 6).

of Prost.[8] This diagram shows the following features :

1 the $N-A_1$ line is throughout second order and terminates at a critical end point Q,

2 there are two tricritical points, viz., R on the A_1-A_2 boundary and P on the $N-A_2$ boundary.

Case 2

If the elastic constants C_1 and C_2 are different and favour an easy compression of ψ_1 (i.e., δB_1 increases and δB_2 decreases), then at small values of Z^2, a new first order phase boundary separating two A phases, viz., A_2 and A_2' (which are distinguished by different values of θ and hence q_0) appears (see Fig. 5.2). For small values of θ, q_0 is of the order K_1 and ψ_1 is much larger than ψ_2. The A_2' phase can be identified with the experimentally observed A_d phase even though ψ_2 is strictly speaking non-zero. (For the purpose of theoretical discussion we shall be referring to it as A_2' in this section.)

For $0 < \theta < \frac{\pi}{2}$, the amplitudes of ψ_1 and ψ_2 are comparable, leading to the A_2 phase. Across the phase boundary between A_2' and A_2, q_0^{-2} and $\sin^2\theta$ exhibit discontinuities which can be evaluated using

$$\psi_1 = \frac{2D_{12}}{B_{12}} (C_2/C_1)^{1/2} \times \cos\theta$$

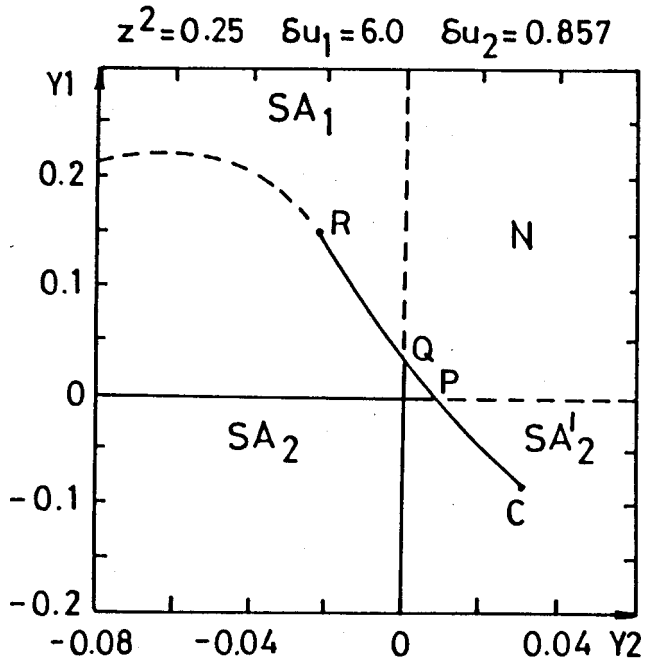

Figure 5.2

Phase diagzam for small incommensurability parameter with asymmetric elastic and fourth ordered terms. The solid line denotes a first order phase boundary while the dashed line denotes a second order boundary.(From Ref.6).

$$\psi_2 = \frac{1}{2} \frac{D_{12}}{B_{12}} \times \sin\theta$$

via

$$\Delta\bar{q}_0^2 = \left(\frac{K_2^2}{4} - K_1^2\right) A(\sin^2\theta).$$

The A_2' - A_2 boundary is a continuation of the first order $N - A_2$ line beyond P (see Fig. 5.2) and terminates at a critical point C where the value of $\Delta\bar{q}_0^2$ goes to zero. In the framework of mean field theory critical fluctuations in the vicinity of C are expected to be similar to those encountered at the liquid-gas critical point. The presence of the critical point C indicates that there is no difference in symmetry between the A_2 and A_2' with different reltive amplitudes of ψ_1 and ψ_2. There is also a tricritical point R on the A_1 - A_2 phase boundary.

Case 3

When either the incommensurability parameter Z^2 is further increased or δB_1 increased and δB_2 decreased another boundary in the form of a first order $A_1 - A_2'$ line appears (Fig. 5.3) terminating at one end in a mean field bicritical point B where the N, A_1 and A; phases meet. The other end of this A_1 - A; line ends at a triple point T where the A,, A_2 and A; phases coexist. The critical point C marking the end of the line distinguishing the

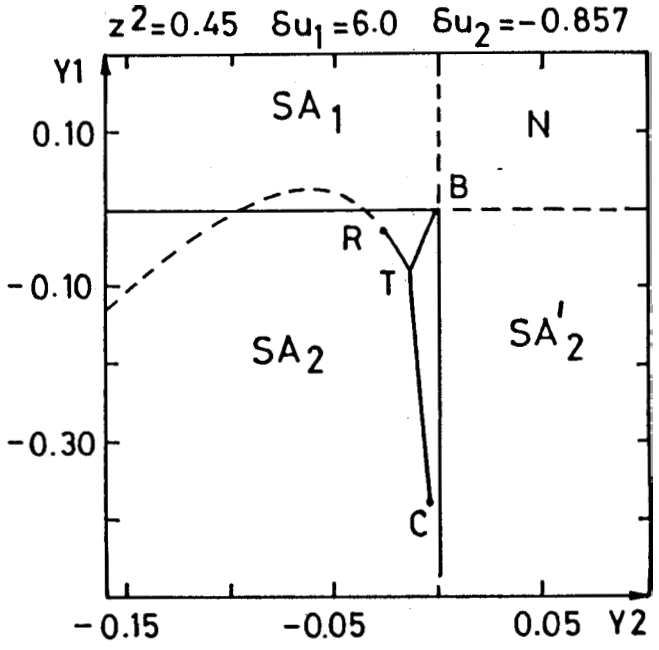

Figure 5.3

Phase diagram for larger incommensurability parameter with asymmetric elastic and fourth ordered terms. The solid line denotes a first order phase boundary, while the dashed line denote4 a second order boundary. (From Ref. 6).

A_2 and A_2' phases continues to exist. The tricritical point R on the $A_1 - A_2$ phase boundary is also retained.

On the experimental side, high resolution X-ray studies of Chan et al.[5] have shown the existence of the $A_1 - A_2$ tricritical point for the hexylphenyl cyanobenzoyloxy benzoate (DB6) and terephthal-bis-butylaniline (TBBA) system. However a tricritical point for the $N - A_2$ transition has not been observed so far. Very recently Shashidhar et al.[3] reported the first observation of the $A_2' - A_2$ (or $A_d - A_2$) critical point in the temperature-concentration diagram of 4-n-undecyloxyphenyl-4'-(4"-cyanobenzyloxy)benzoate (or 11OPCBOB) and 4-n-nonyloxybiphenyl-4'-cyanobenzoate (or 9OBCB) binary system. Their results showed that the first order $A_2' - A_2$ boundary, characterised by a narrow two-phase region (in which the density modulations of both A_2' and A_2 coexist) terminates at a critical point. The difference in the wavevector q_0 and q_0' at the $A_2' - A_2$ transition was found to decrease with an accompanying decrease in the width of the two-phase region as the critical point was approached.

Earlier Studies on the $A_1 - N_{re} - A_d$ Point

We shall now summarize the situation concerning the $A_1 - N_{re} - A_d$ bicritical point. Several experimental binary phase diagrams exhibiting the $A_1 - N_{re} - A_d$ point have been reported[1,11] (see Fig. 5.4). It has also been pointed out[12] that the global topology

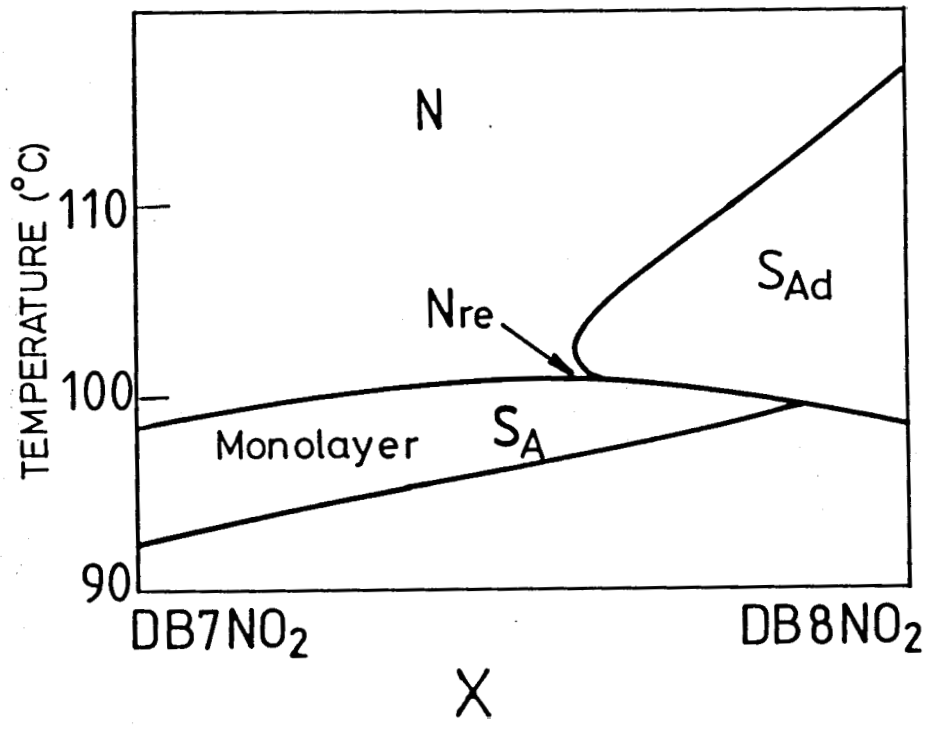

Figure 5.4

Binary phase diagram showing A, -N_{re} - A_d point. (From Ref. 1).

of these phase diagrams near the $A_1 - N_{re} - A_d$ point is similar to the typical topology of a magnetic bicritical point[13,14] (see Fig. 5.5). However, it is well known from the studies on the nematic-smectic A-smectic C (NAC) multicritical point[15-17] that the true topology of the phase diagram can be observed only in the immediate vicinity of the NAC point. No such high resolution experimental studies have been carried out near the expected $A_1 - N_{re} - A_d$ point. On the theoretical side, although the mean field theory discussed above predicts a bicritical point, when the effect of the fluctuations are considered, the very existence of such a point becomes questionable. It has been argued that since both A_d and A_1 phases have the same symmetry, the $N-A_d$ and $N-A_1$ transitions should both belong to the same universality class, i.e., the inverted xy universality class.[18] Renormalization group calculations[13,19] show that under such a circumstance the resulting multicritical point should in fact be a tetracritical point and not a bicritical point. It has also been predicted[20] that an offshoot of this situation would be an incommensurate A phase with both A_d- and A_1-like modulations. In view of these a high resolution study of the phase diagram near the $A_1 - N_{re} - A_d$ point has been taken up along with the detailed calorimetric (DSC) investigations. The results of these studies which are described in the following have led us to postulate a new alternative for the $A_1 - N_{re} - A_d$ bicritical point.

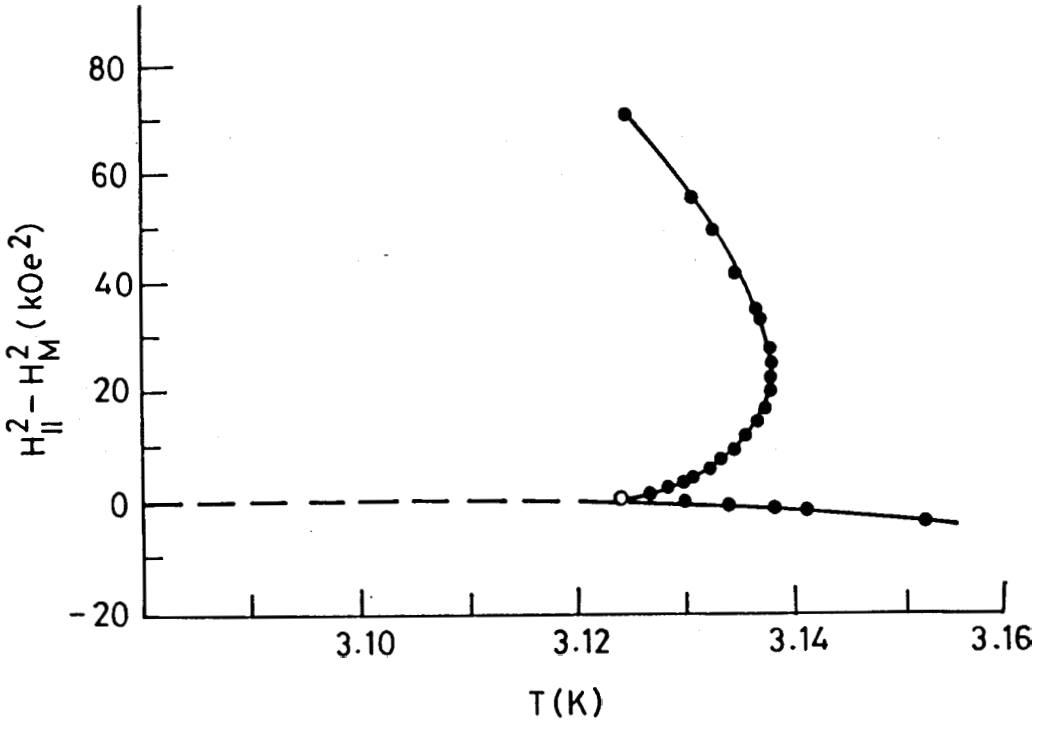

Figure 5.5

True bicritical topology been in magnetic systems.
(From ref. 14).

5.3 A NEW ALTERNATIVE FOR THE $A_1 - N_{re} - A_d$ BICRITICAL POINT

5.3.1 Experimental

As remarked before, a careful evaluation of topology of the phase diagram near the $A_1 - N_{re} - A_d$ point involves collection of data with as high a precision in concentration and temperature as possible. The major difficulty that was encountered in achieving such an accuracy in concentration was the non-availability of materials in sufficient quantities. It is evidently not difficult to achieve a precision of 0.01% or even better when large quantities of the sample are available. In our case, however, the quantity of the substances available was only about 200-250 mg. of each material. With this limited quantity it was imperative to make at least 25-30 individual mixtures, each mixture with as high an accuracy as possible, to obtain enough data to map a high resolution diagram. This was achieved in the following manner.

A) Weighing

A Perkin-Elmer AD2 microbalance with a weighing accuracy of 1 microgram was used. Care was taken to mount the balance on a massive supporting table so that vibrations did not drastically affect the stability of the balance. The constancy in the reading of the balance for any given weighing depends on a number of parameters like constancy of room temperature, the humidity of the atmosphere and the time for which the balance is allowed to equi-

libriate. The effect of these factors were minimised by accurately controlling the ambient temperature and humidity and waiting for long periods (2-3 hr.) before any reading of the balance was taken for each weighing. Despite these precautions it was observed that the balance reading was never truly constant. There was a small but perceptible drift. This problem was overcome by analysing the amount of drift with time. Typically, for instance, after waiting for a period of about 2 hours or more, a drift of 1 microgram per hour was observed. The extent of this drift became even less after waiting for still longer intervals. An evaluation of the drift as a function of waiting period permitted us to obtain the correct weight when extrapolated to zero drift. In this manner it was possible to obtain a weighing accuracy of ±1 microgram and hence a concentration accuracy of about ±0.04 mol % for each mixture.

B) Sample preparations

Requisite amounts of the sample were taken on a glass coverslip. Samples were added very slowly and in very small amounts so as to minimise mechanical disturbances. Care was taken to see that these samples are lumped together at the centre of the coverslip. Even if a small speck stays out from the bulk it leads to uncertainties in the concentration determination. To ensure good thermal diffusion, the substance with a lower melting point was

first weighed on to the coverslip on the top of which the second sample (with a higher melting point) was added. The coverslip with the sample was then transferred carefully onto a hot stage and the substances were mixed thoroughly. The hot stage has been previously maintained at a suitable temperature so that the substance melts as soon as the coverslip is transferred on to it - this ensures a homogeneous mixing. The mixture prepared in this way was then used for optical microscopic studies. For this purpose, the sample was taken in a molten state from the mixture and was transferred on to a slide. The transition temperatures were determined using a Leitz-Orthoplan microscope in conjunction with a Mettler FP82 hot stage. The sharpness of the transition was used as a measure to test the homogeneity of the mixture. Whenever the transition was found to be rather broad, that mixture was discarded. Also at least 3 or more slides were prepared from the same 'mother mixture[1] and their transition temperatures were examined. If the slides showed differences in the transition temperatures this was attributed to a concentration gradient in the mixture and the mother mixture was not used for the experiment. Only those mixtures which showed repeatedly reproducible transition temperatures were considered for high resolution phase diagram studies. Preliminary observations were carried out using a heating/cooling rate of 1°C/min. To determine the exact transition temperature we used a rate of 0.1°C/min, the lowest rate possible with the Mettler (FP82) controller. Although the displayed read-

ing on the Mettler hot stage was 100 mK, we could, by using a digital timer synchronously in conjunction with the hot stage, obtain (by interpolation) a temperature reading accuracy of ± 20 mK.

C) Materials

The constituent compounds of the binary system studied are 4-n-octyloxyphenyl - 4'-(4"-nitrobenzoyloxy)benzoate (DB8.O.NO_2) and 4-n-decyloxyphenyl-4'-(4"-nitrobenzoyloxy)benzoate (DB10.O.NO_2). The chemical structures of the compounds and the transition temperatures are given in Fig. 5.6. DB8.O.NO_2 shows N, A_1 and $\tilde{C}$ phases while DB10.O.NO_2 shows N, A_d, $\tilde{C}$ and C_2 phases.

D) DSC Studies

The calorimetric studies were performed using a differential scanning calorimeter, DSC-4 (Perkin-Elmer). It was used in conjunction with a fully computerised Thermal Analysis Data Station (TADS) which permitted automatic data acquisition as well as analysis using standard software programs. The instrument was calibrated using pure Indium before and after any set of experiments.

E) X-ray Studies

The X-ray diffraction experiments were carried out using a computer controlled Guinier diffractometer (Huber 6 4 which

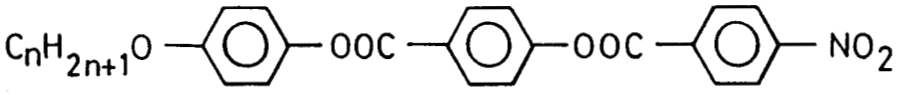

(n = 8)

4-n- octyloxyphenyl-4'-(4''-nitrobenzoyloxy) benzoate

(DB8.O.NO_2)

I $\xrightarrow{227\ °C}$ N $\xrightarrow{130\ °C}$ A_1 $\xrightarrow{109\ °C}$ $\tilde{C}$ $\xrightarrow{86.4°C}$ K

(n=10) (DB 10.O.NO_2)

4-n- decyloxyphenyl - 4'-(4''-nitrobenzoyloxy) benzoate

I $\xrightarrow{220\ °C}$ N $\xrightarrow{210.8\ °C}$ A_d $\xrightarrow{119\ °C}$ $\tilde{C}$ $\xrightarrow{107.4\ °C}$ C_2 $\xrightarrow{89\ °C}$ K

Figure 5.6

***Chemical** formulae for n-alkoxyphenyl-4'-(4''-nitrobenzoyloxy)benzoate (n = 8 and 10). Their transition temperatures are also given.*

has already been described in Chapter II. We shall only be giving here a few relevant facts. The sample was taken in a 0.5 mm diameter Lindemann glass capillary whose ends were then sealed. A monodomain sample was obtained by cooling in the presence of a 2.4T magnet. The accuracy in the determination of the wavevector at any temperature was 2×10^{-4} $\mathring{A}^{-1}$, while the temperature was maintained constant to ± 10 mK during any measurement.

5.3.2 **Results and Discussion**

The complete temperature-concentration (T - X) diagram is shown in Fig.5.7 which shows a $A_1 - N_{re} - A_d$ point for X = 55 mol % of $DB10.O.NO_2$. It must be remarked that this diagram has been obtained by optical observation of the textures under a polarising microscope (Leitz-Orthoplan). The $A_1 - A_d$ transition was observable as a sudden adjustment of the edges of the focal conics. It is seen that the global topology of our phase diagram (Fig. 5.7) near the $A_1 - N_{re} - A_d$ point resembles, as in the case of earlier studies,[1,11] the typical topology seen near a magnetic bicritical point. However, we shall show in the following that a completely different picture emerges when we examine the high resolution diagram.

The high resolution data (obtained with a precision of ±0.04 mol% in X and i20 mK in T) in the immediate vicinity of the $A_1 - N_{re} - A_d$ point are presented in Fig. 5.8. By definition,

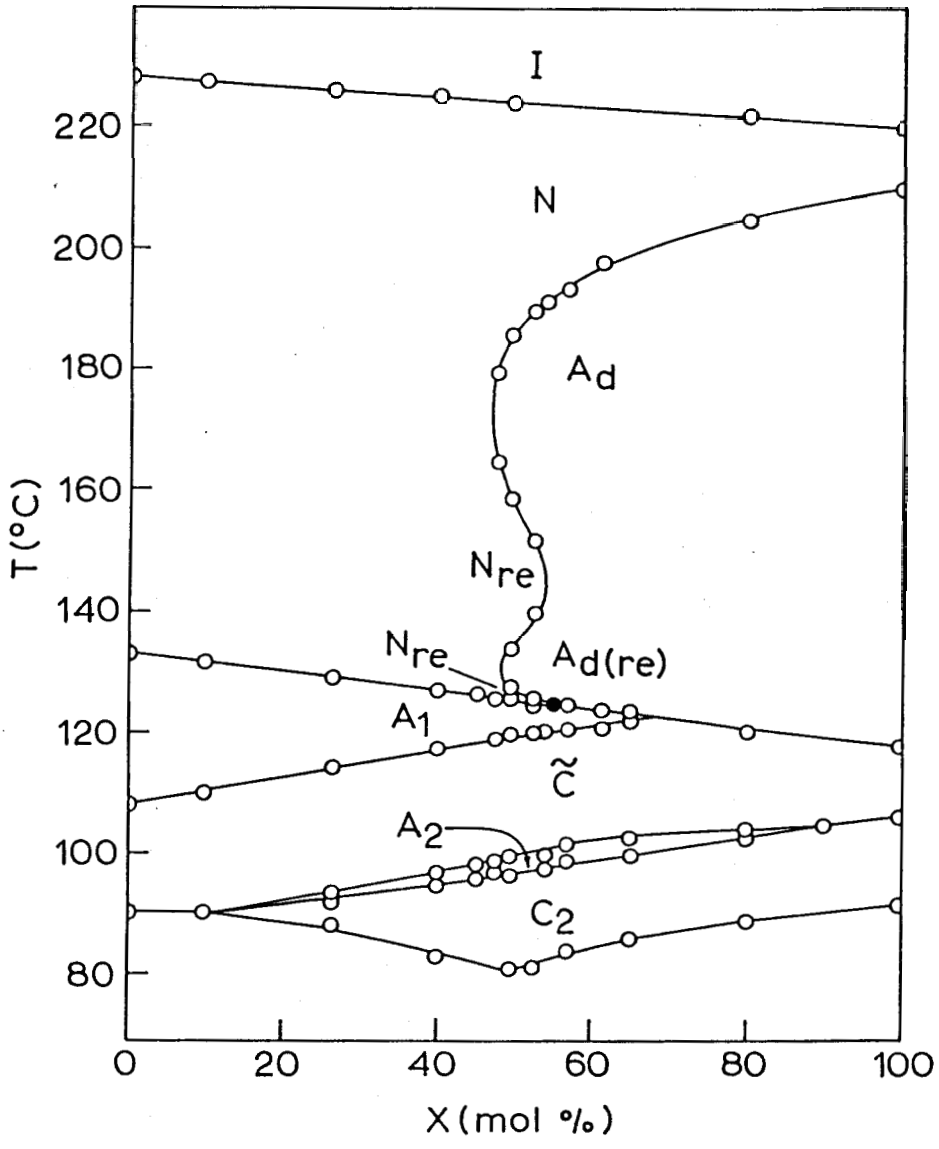

Figure 5.7

Complete temperature-concentration diagram for binary mixtures of DB8.O.NO$_2$ and DB10.O.NO$_2$. X is the mol % of DB10.O.NO$_2$ in the mixture. The solid lines are guides to the eye. The A_1-N_{re}-A_d point which occurs at X = 55.0 is denoted by a closed circle. The size of the circle constitute4 approximatetq the entire region of T over which the high resolution data are shown in Fig. 5.8. (For explanation of the various phases, see Ref. 1.).

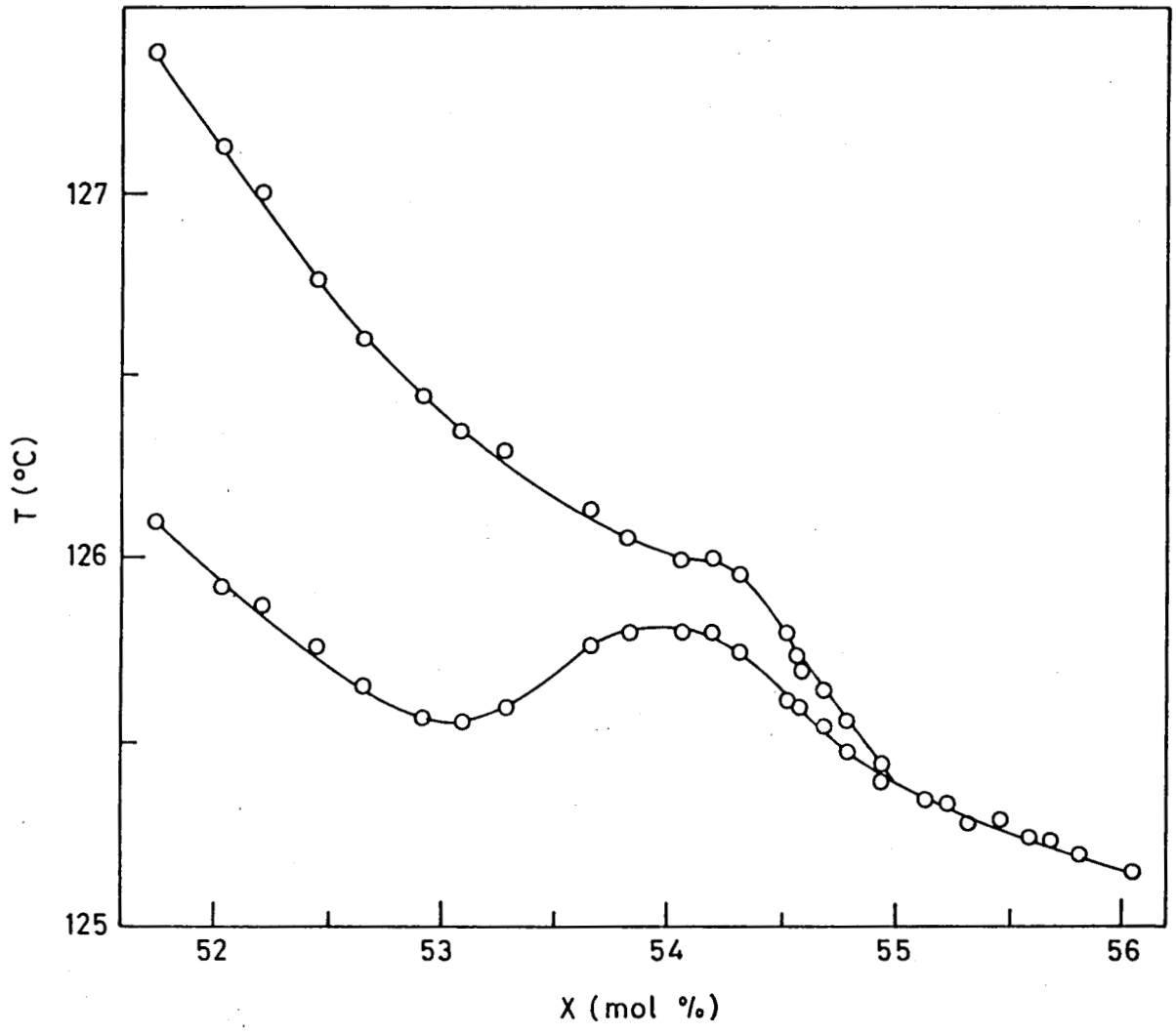

Figure 5.8

High** resolution. T-X diagram **in the vicinity of the** A, -N_{re}-A_d **point.** **The solid line6 are guide to the eye.

at the bicritical point, the two second-order boundaries should come in tangentially to the first-order phase boundary.[10,12] Also, the heat associated with the first-order transition should go to zero at the bicritical point. The high resolution phase diagram (T-X) (Fig. 5.8) shows that the first of the above requirements is not satisfied - the second order $A_d - N_{re}$ boundary does not appear to be tangential to the first order $A_d - A_1$ boundary. To verify if the heat associated with the $A_d - A_1$ transition goes to zero at the $A_1 - N_{re} - A_d$ point we have taken up detailed differential scanning calorimetry studies. The results of these studies are described below.

Initial DSC studies conducted for concentrations on either side of the $A_1 - N_{re} - A_d$ point showed that both $N_{re} - A_1$ and $A_1 - A_d$ transitions show clear signatures in their DSC runs while the $A_d - N_{re}$ transition was undetectable. This result is in conformity with the recent high resolution AC calorimetric study[21] wherein it was observed that the anomalous specific heat signal for the $N_{re} - A_1$ transition was very much greater than that for the $A_d - N_{re}$ transition.

In all 8 mixtures (X = 55.13, 55.37, 55.72, 56.02, 56.97, 57.83, 58.91 and 60.79) exhibiting the $A_1 - A_d$ transition and 7 mixtures (X = 49.99, 51.95, 53.52, 53.92, 54.39, 54.73 and 54.92) showing the $A_1 - N_{re}$ transition were studied. For each concentration

DSC runs were taken at 10 different rates, ranging from 1.0°C/min to 0.1°C/min, the lowest rate possible with the DSC set up. The total area under the endothermic peak was calculated using the computerised TADS system and the corresponding enthalpy (ΔH) was evaluated for each heating rate. The transition enthalpy includes both the latent heat and the specific heat contributions. The value of AH obtained in this manner is shown in Fig. 5.9 as a function of heating rate for a few representative concentrations. These data in fact constitute the average of at least 2 different heating runs taken for each heating rate. A least-squares-fit of the AH data to a straight line was carried out which gave $(\Delta H)_0$, the enthalpy extrapolated to zero heating rate. Although in principle, DSC cannot differentiate between rapidly varying entropy and the true latent heat of transition, we believe that the value of $(\Delta H)_0$ evaluated in this manner should be very close to the latent heat of transition. It may be recalled that very recently Ratna and Chandrasekhar[22] have ascertained the efficacy of this technique by studying the A-N and nematic-isotropic (N-I) transitions of 4-n-octyloxy-4'-cyanobiphenyl (8OCB) for which adiabatic calorimetry data are available.

We shall now examine the plots of AH vs. heating rate for different concentrations. For the $A_1 - A_d$ transition (see Figs. 5.9a and b) the value of AH is seen to be independent of the heating rate, as is generally expected for first order transitions

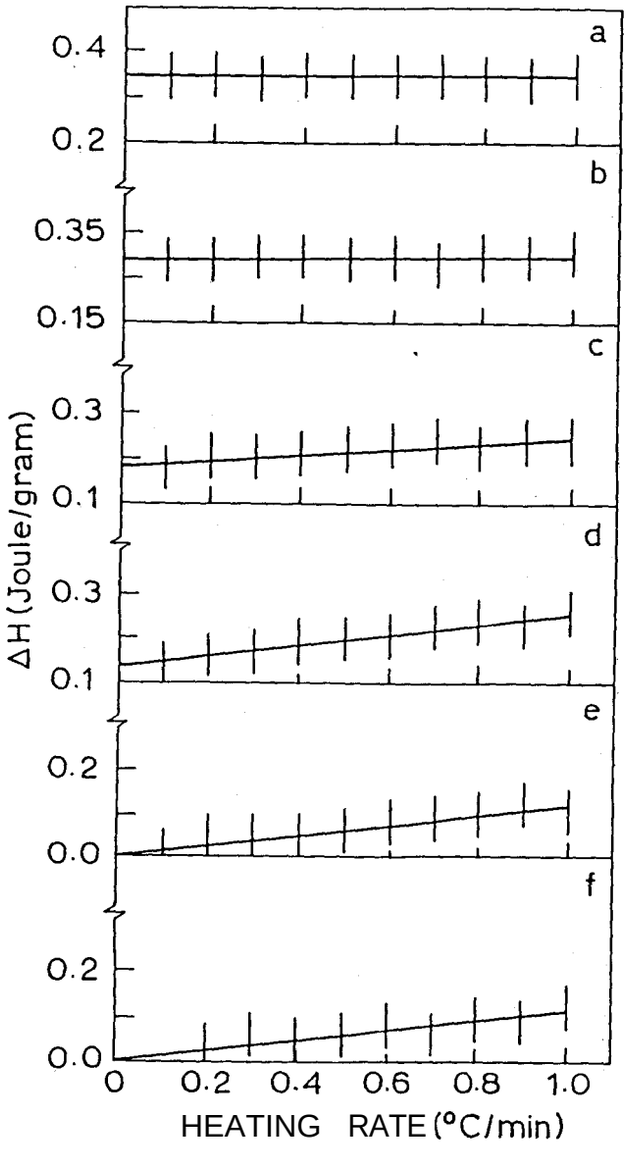

Figure 5.9. *Plots of enthalpy (ΔH) vs. heating rate for the A_1-A_d (a, b), and A_1-N_{re} transitions (c-f) as obtained by DSC run4 for different concentrations. The values of X are (a) 56.02, (b) 55.13, (c) 54.92, (d) 54.73, (e) 51.95, and (f) 49.99. Each data point is shown as a vertical line whose height represents the error bar in the determination of AH. The solid line is a least-square-fit of the data to a straight line. The same fit also gives $(\Delta H)_0$, the enthalpy extrapolated to zezo heating rate, which can be equated to the Patent heat of transition.*

with little or no pretransitional effects.[23] In the case of $A_1 - N_{re}$ transition, AH is strongly dependent on the heating rate. For some concentrations (see Figs. 5.9c & d), $(\Delta H)_0$ is seen to be non-zero implying that the transition is weakly first order with large pretransitional effects. On the other hand, for some other mixtures (Figs. 5.9e & f) $(\Delta H)_0 \approx 0$ signifying that the $A_1 - N_{re}$ transition for these concentrations is probably second order. The complete data on $(\Delta H)_0$ for all the concentrations are plotted against the concentration (X) in Fig. 5.10. The following important features are clear from the diagram :

i) Although $(\Delta H)_0$ for the $A_1 - A_d$ transition decreases initially with decreasing X, it does not go to zero at X = 55.0, the concentration at which the $A_1 - N_{re} - A_d$ point occurs. We can therefore infer that the $A_1 - N_{re} - A_d$ point is not a bicritical point.

ii) The $A_1 - N_{re}$ boundary is seen to be of second order at low concentrations but becomes first order on approaching the $A_1 - N_{re} - A_d$ point. Hence, there should be a tricritical point on the $A_1 - N_{re}$ line.

X-ray Studies

Our DSC results have shown that the $A_d - A$, transition is of first order in nature. The signature of this transition in

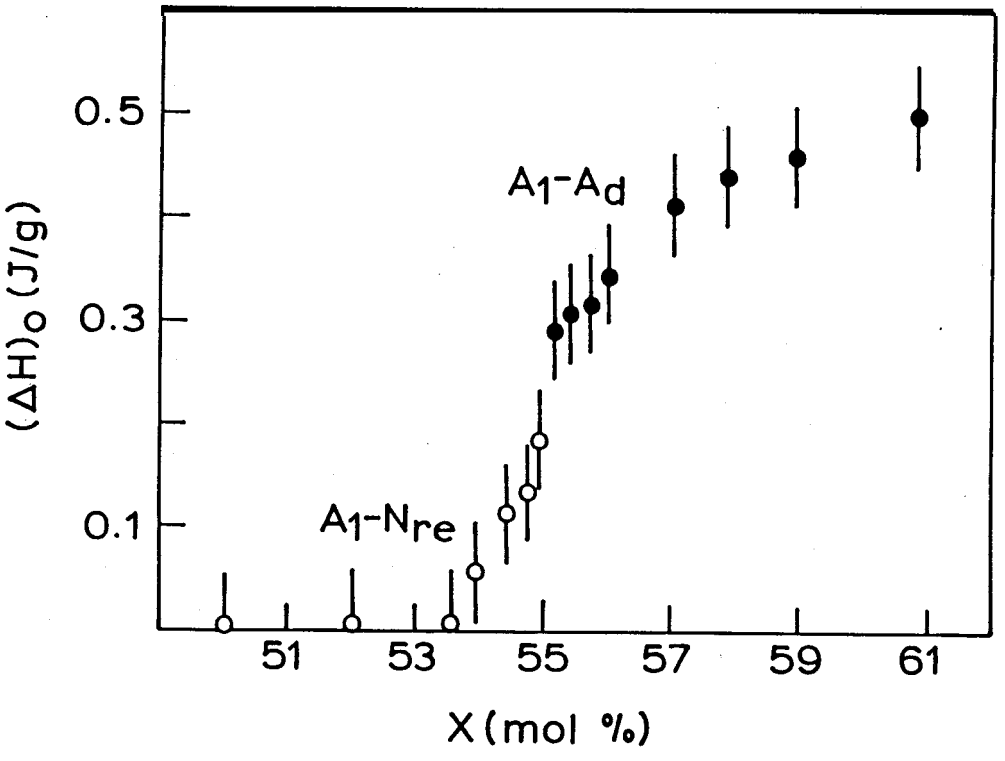

Figure 5.10

Plot of latent heat $(\Delta H)_0$ *associated with the* A_1-A_d (•) *and* A - N_{re} (o) *transitions in the neighbourhood of the* A_1-N_{re}-A_d *point.*

X-ray studies should be a jump in the layer spacing whose magnitude should go to zero at the bicritical point. It is of interest to see if such a behaviour can be seen on approaching the $A_1 - N_{re} - A_d$ point. With this in view we have conducted X-ray studies (using the diffractometer set up described in Chapter II) of the $A_1 - A_d$ transition for several concentrations near the $A_1 - N_{re} - A_d$ point. Data for two representative concentrations, viz., X = 55.37 and 56.01 are shown in Figs. 5.11 and 5.12 respectively. It is seen that essentially a similar behaviour of the layer spacing (d) is seen for both the concentrations. Starting from the A_d phase, d increases with decrease of temperature and at the $A_d - A_1$ transition a clear jump in d is observed. (It may be recalled that a similar jump in d has been seen earlier for other systems exhibiting the $A_1 - A_d$ transition.[4,11,24]) This jump is about 15.5 Å for X = 55.37 and 16 Å for X = 56.01 - there is no pronounced decrease in the magnitude of the jump in d as the $A_1 - N_{re} - A_d$ point is approached. Hence our X-ray data also support the deduction of the DSC results and the high resolution T-X diagram, viz., the $A_1 - N_{re} - A_d$ point is not a bicritical point.

Also, as mentioned in Section 5.1, the renormalisation group theory predicts the existence of an incommensurate phase near the $A_1 - N_{re} - A_d$ point. However, neither optical nor X-ray results showed any indication of such a phase even for concentrations within 0.1 mol % of the concentration at which the $A_1 - N_{re} - A_d$

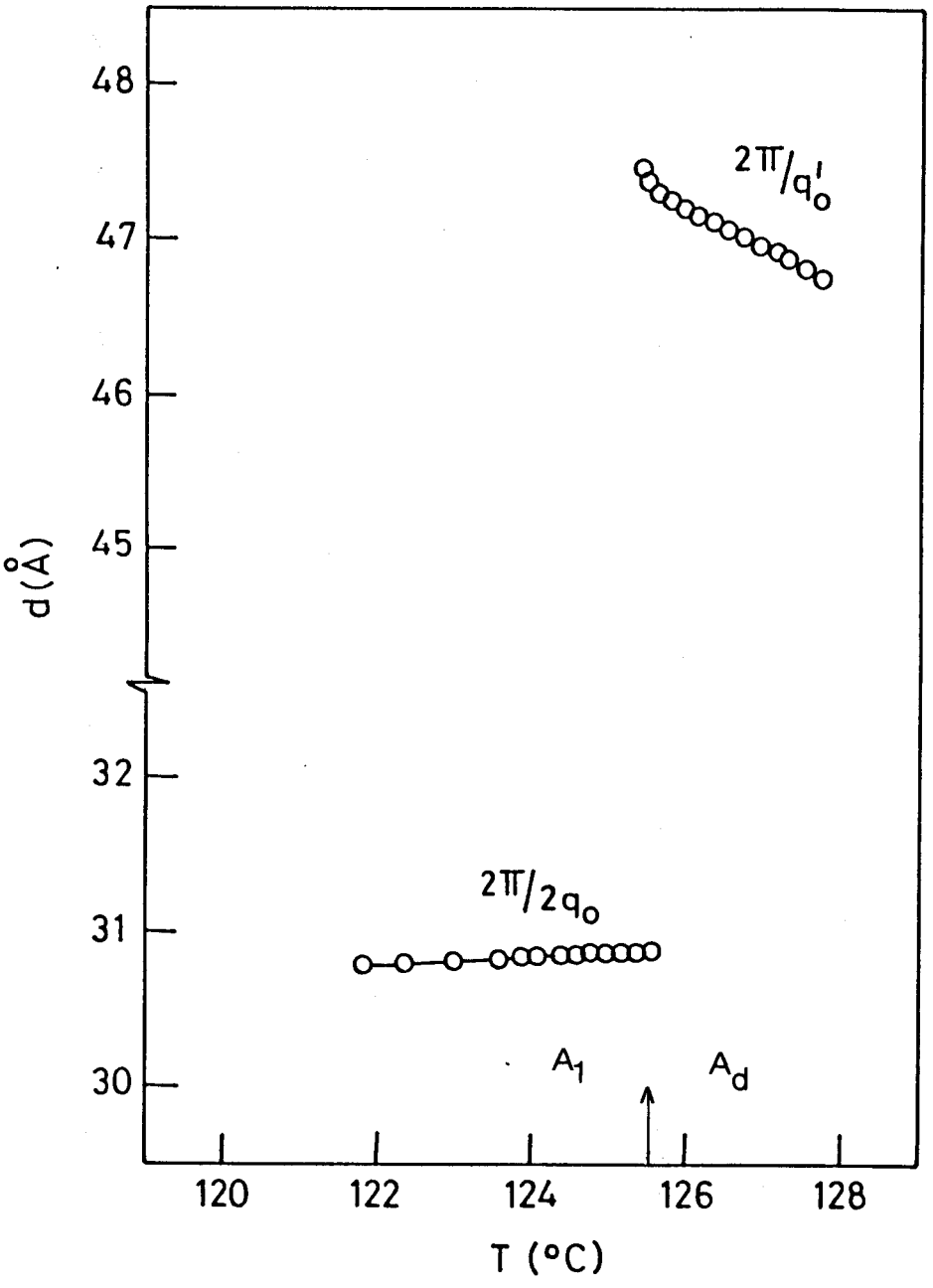

Figure 5.11

Thermal vaiiation of the layer spacing for X = 55.37 mol % of DB10.O.NO_2.

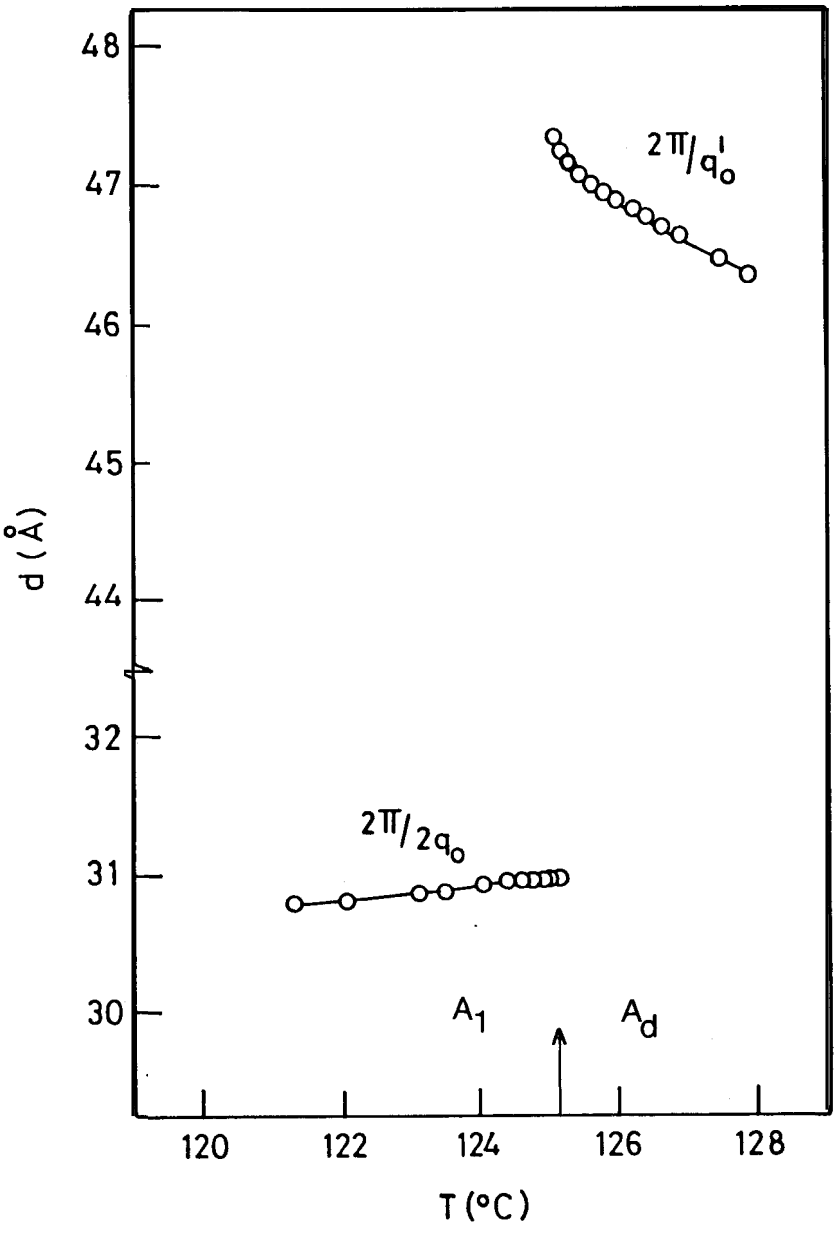

Figure 5.12

***Layer** spacing variation **with temperatute** seen for X = 56.01 mol % of DB10.O.NO_2.*

point exists. Thus a tetracritical point can be ruled out. The question therefore arises as to the nature of the $A_1 - N_{re} - A_d$ point. The results of our DSC studies described earlier show that the $A_d - N_{re}$ phase boundary is second order throughout while the $A_1 - N_{re}$ boundary is second order away from the $A_1 - N_{re} - A_d$ point, but becomes first order close to it.

Thus we can infer that the $A_1 - N_{re} - A_d$ bicritical point has split into a critical end point (for the $A_d - N_{re}$ boundary) and a tricritical point (on the $A_1 - N_{re}$ boundary). Such a situation has indeed been postulated theoretically in magnetic systems,[25,26] but has not yet been envisaged in the theory of frustrated smectics. It must be mentioned that the accuracy in the determination of $(\Delta H)_0$ which is ±0.05 J/gm, is not sufficient for us to exactly locate the concentration at which the tricritical point occurs on the $A_1 - N_{re}$ line. The possibility that the tricritical point may lie very close to or at the critical end point itself cannot be completely ruled out either. In the case of the latter, the $A_1 - N_{re} - A_d$ point would be a new kind of multicritical point which has again been considered theoretically in anisotropic ferromagnets.

Very recently Prost and Toner,[27] using dislocation loop theory of the A–N transition, have predicted that a first order $A_d - A_1$ phase boundary can terminate either at a critical point or as a nematic island which exists in a sea of smectic A separated

from another nematic, referred to as 'main domain' nematic. Under certain conditions the theory predicts that this nematic island can join the main domain nematic and thereby lead to an unusual phase diagram as shown in Fig. 5.13. It is interesting to note that some of the topological features of the theoretical diagram appear to be qualitatively similar to our phase diagram (see Fig. 5.8). Clearly further studies, experimental as well as theoretical, are needed before we can generalise the situation concerning the $A_1 - N_{re} - A_d$ point.

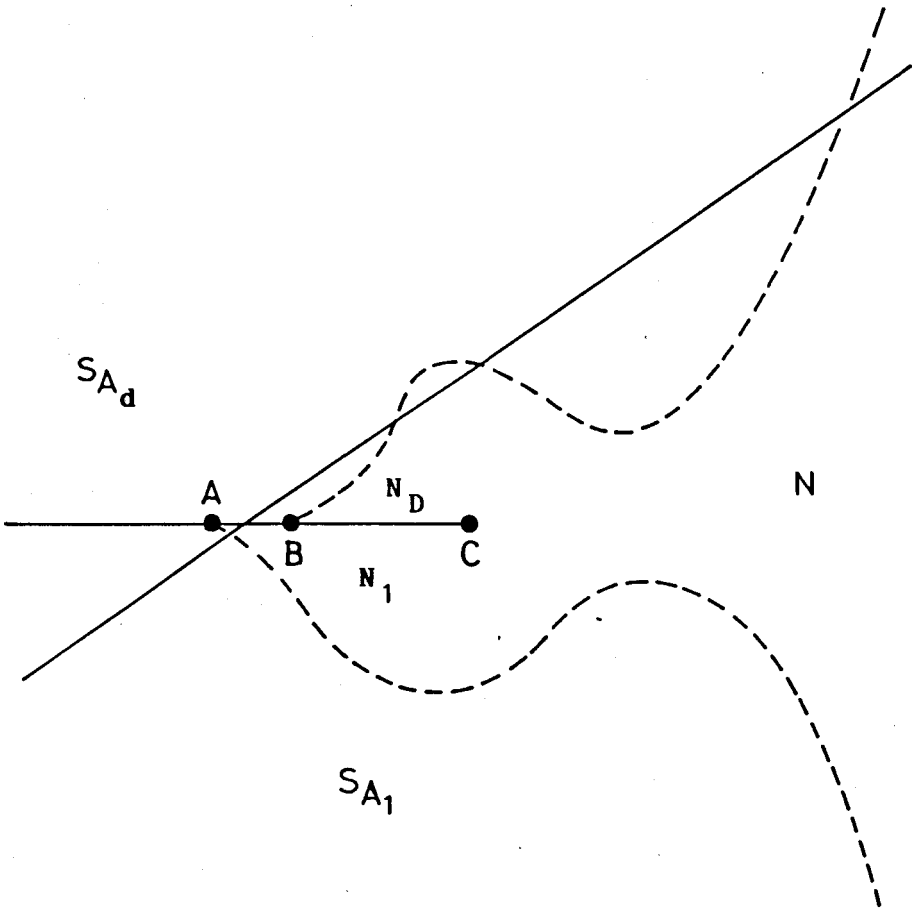

Figure 5.13

Theoretical phase diagram showing the N_d-N, critical point C and two critical end points, A (for the A_1N_1 line) and B (for the A_dN_d line). (From Ref. 27).

REFERENCES

1 F. Hardouin,A.M.Levelut, M.F.Achard and G.Sigaud, J.Chim. Phys., 80, 53 (1983)

2 B.R.Ratna, R.Shashidhar and V.N.Raja, Phys. Rev. Lett., 55, 1476 (1985)

3 R.Shashidhar, B.R.Ratna, S.Krishna Prasad, S.Somasekhara and G.Heppke, Phys. Rev. Lett., 59, 1209 (1987)

4 A.M.Levelut, R.J.Tarento, F.Hardouin, M.F.Achard and G. Sigaud, Phys. Rev. A, 24, 2180 (1981)

5 K.K.Chan, P.S.Pershan, L.B.Sorensen and F.Hardouin, Phys. Rev. A, 34, 1420 (1986); Phys. Rev. Lett., 54, 1694 (1985)

6 P. Barois, J. Prost and T.C.Lubensky, J. de Phys., 46, 391 (1985)

7 L.D.Landau and E.M.Lifshitz, Statistical Physics, Part I (Pergamon, New York, 1982), p. 468.

8 J. Prost, J. de Phys., 40, 581 (1979)

9 J. Prost, in "Liquid Crystals of One- and Two-Dimensional Order", Eds. W.Helfrich and G.Heppke (Springer-Verlag, Berlin, 1980), p. 125

10 J. Prost and P. Barois, J. Chim. Phys., 80, 65 (1983)

11 F. Hardouin, M.F.Achard, Nguyen Huu Tinh and G. Sigaud, Mol. Cryst. Liq. Cryst. Lett.,3, 7 (1986)

12 J. Prost, Advances in Physics, 33, 1 (1984)

13 J.M.Kosterlitz, D.R.Nelson and M.E.Fisher, Phys. Rev. B, 13, 412 (1976)

14 Y.Shapira, "Multicritical Phenomena", eds. R.Pynn and A.Skjeltrop (Plenum Press, New York and London, 1983), p. 35.

15 D.Brisbin, D.L.Johnson, H.Fellner and M.E.Neubert, Phys. Rev. Lett., 50, 178 (1983)

16 R.Shashidhar, B.R.Ratna and S.Krishna Prasad, Phys. Rev. Lett., 53, 2141 (1984)

17 S.Somasekhara, R.Shashidhar and B.R.Ratna, Phys. Rev. A, 34, 3561 (1986)

18 C. Das Gupta and B.F.Halperin, Phys. Rev. Lett., 47, 1556 (1981); J. Toner, Phys. Rev. B, 26, 462 (1982); see also T.C.Lubensky, J. Chim. Phys., 80, 31 (1983)

19 M.E.Fisher and D.R.Nelson, Phys. Rev. Lett., 32, 1350 (1974)

20 J. Wang, "The Frustrated Smectic Phases in Liquid Crystals", Ph. D. Thesis, University of Pennsylvania, 1985

21 J.O.Indekeu, A. Nihat Berker, C.Chiang and C.W.Garland, Phys. Rev. A, 35, 1371 (1987)

22 B.R. Ratna and S.Chandrasekhar, Mol. Cryst. Liq. Cryst. (to be published)

23 R. De Hoff, R. Biggers, D. Brisbin and D.L.Johnson, Phys. Rev. A, **25**, 472 (1982)

24 P.E.Cladis and H.R.Brand, Phys. Rev. Lett., **52**, 2261 (1984)

25 H. Rohrer, A.Aharony and S.Fishman, J. Magn. and Magn. Mat., **15**, 396 (1980)

26 S.Galam and A.Aharony, J. Phys. C-Solid State Phys., **13**, 1065 (1980)

27 J. Prost and J. Toner, Phys. Rev. A, **36**, 5008 (1987).